NeuroImage: Clinical 24 (2019) 101942

Contents lists available at ScienceDirect

NeuroImage: Clinical

journal homepage: www.elsevier.com/locate/ynicl

Increased brain responsivity to galvanic vestibular stimulation in bilateral vestibular failure

Christoph Helmchen[a,*], Matthias Rother[a], Peer Spliethoff[a], Andreas Sprenger[a,b]

[a] Department of Neurology, University of Lübeck, University Hospitals Schleswig-Holstein, Campus Lübeck, Ratzeburger Allee 160, 23538 Lübeck, Germany
[b] Institute of Psychology II, University of Luebeck, Germany

ARTICLE INFO

Keywords:
Bilateral vestibulopathy
Galvanic vestibular stimulation
Visual-vestibular interaction
fMRI

ABSTRACT

In this event-related functional magnetic resonance imaging (fMRI) study we investigated how the brain of patients with bilateral vestibular failure (BVF) responds to vestibular stimuli. We used imperceptible noisy galvanic vestibular stimulation (GVS) and perceptible bi-mastoidal GVS intensities and related the corresponding brain activity to the evoked motion perception. In contrast to caloric irrigation, GVS stimulates the vestibular organ at its potentially intact afferent nerve site.

Motion perception thresholds and cortical responses were compared between 26 BVF patients to 27 age-matched healthy control participants. To identify the specificity of vestibular cortical responses we used a parametric design with different stimulus intensities (noisy imperceptible, low perceptible, high perceptible) allowing region-specific stimulus response functions. In a 2 × 3 flexible factorial design all GVS-related brain activities were contrasted with a sham condition that did not evoke perceived motion.

Patients had a higher motion perception threshold and rated the vestibular stimuli higher than the healthy participants. There was a stimulus intensity related and region-specific increase of activity with steep stimulus response functions in parietal operculum (e.g. OP2), insula, superior temporal gyrus, early visual cortices (V3) and cerebellum while activity in the hippocampus and intraparietal sulcus did not correlate with vestibular stimulus intensity. Using whole brain analysis, group comparisons revealed increased brain activity in early visual cortices (V3) and superior temporal gyrus of patients but there was no significant interaction, i.e. stimulus-response function in these regions were still similar in both groups. Brain activity in these regions during (high)GVS increased with higher dizziness-related handicap scores but was not related to the degree of vestibular impairment or disease duration. nGVS did not evoke cortical responses in any group.

Our data indicate that perceptible GVS-related cortical responsivity is not diminished but increased in multisensory (visual-vestibular) cortical regions despite bilateral failure of the peripheral vestibular organ. The increased activity in early visual cortices (V3) and superior temporal gyrus of BVF patients has several potential implications: (i) their cortical reciprocal inhibitory visuo-vestibular interaction is dysfunctional, (ii) it may contribute to the visual dependency of BVF patients, and (iii) it needs to be considered when BVF patients receive peripheral vestibular stimulation devices, e.g. vestibular implants or portable GVS devices. Imperceptible nGVS did not elicit cortical brain responses making it unlikely that the reported balance improvement of BVF by nGVS is mediated by cortical mechanisms.

1. Introduction

Bilateral vestibular failure (BVF) is a severe chronic disorder of the labyrinth or the eighth cranial nerve characterized by unsteadiness of gait and oscillopsia during head movements. The diagnostic criteria of BVF have recently been revised by the Barany Society (Strupp et al., 2017). BVF has a wide spectrum of etiologies (Zingler et al., 2007). In most patients the reason remains (Cutfield et al., 2014) unclear (idiopathic) but many patients suffer from ototoxic drugs (e.g. aminoglycosides, amiodarone). Oscillopsia and blurred vision during head movements and locomotion result from a deficient vestibulo-ocular reflex (VOR) which normally stabilizes gaze during rapid head movements. Unfortunately, about 80% of BVF patients do not recover, particularly since peripheral vestibular nerve cell regeneration is poor

* Corresponding author at: Department of Neurology, University of Lübeck, University Hospitals Schleswig-Holstein, Campus Lübeck, Ratzeburger Allee 160, D-23538 Lübeck, Germany.
E-mail address: christoph.helmchen@neuro.uni-luebeck.de (C. Helmchen).

https://doi.org/10.1016/j.nicl.2019.101942
Received 27 December 2018; Received in revised form 31 May 2019; Accepted 17 July 2019
Available online 19 July 2019

(Zingler et al., 2008).

Non-vestibular mechanisms have been suggested to provide central vestibular compensation in BVF, e.g., substitution by upregulation of the gain in the somatosensory (Strupp et al., 1998), the proprioceptive (Cutfield et al., 2014) or visual system (Dieterich et al., 2007). Accordingly, vestibular deafferentation induces several plastic functional (Becker-Bense et al., 2014; Bense et al., 2004a; Helmchen et al., 2014) and structural (Helmchen et al., 2009; Helmchen et al., 2011; zu Eulenburg et al., 2010) changes in the brain. It is a matter of debate whether these changes are clinically beneficial, subserve vestibular compensation or purely reflect the consequence of a lack of vestibular input (maluse, disuse). Compensatory mechanisms in BVF are confined to adaptive mechanisms of sensory substitution, i.e. by changing thresholds of other sensory processing and/or reciprocal intersensory interaction (Bense et al., 2004b; Deutschlander et al., 2008; Dieterich et al., 2007; Kalla et al., 2011).

Using brain imaging techniques, cortical visuo-vestibular reciprocal inhibition has been identified as an important mechanism to reduce visual blurring during vestibular activation (e.g. during nystagmus or head movements) or to reduce motion perception during visual stimulation (Brandt et al., 1998). In a meta-analysis considering 28 PET and fMRI studies employing vestibular stimuli in healthy subjects the cytoarchitectonic area OP2 in the parietal operculum was identified as the primary candidate for the human vestibular cortex, i.e., the human homologue of the “parieto-insular vestibular cortex” (PIVC) in macaque monkeys (Zu Eulenburg et al., 2011). In BVF patients, PET brain imaging (H_2O^{15}) during vestibular caloric stimulation revealed decreased activation in PIVC compared to healthy controls (Bense et al., 2004b). Moreover, resting state activity has been examined in patients with vestibular failure to look at more fundamental changes of functional connectivity during the course of the disease. In patients with unilateral vestibulopathy, functional connectivity in neigbouring supramarginal gyrus at the temporo-parietal junction was reduced which partially reversed over a period of three months when patients had improved (Helmchen et al., 2014). BVF patients showed lower connectivity in the posterior insula and parietal operculum that correlated with adaptive changes of the vestibulo-ocular reflex (VOR) (Gottlich et al., 2014). This suggests that connectivity within the visuo-vestibular interaction is impaired which has been suspected by reduced mutual activation in visual and vestibular processing brain regions during caloric irrigation of BVF patients using PET (Bense et al., 2004b).

However, stimulating a severely impaired end organ is probably not sufficient to identify the functional integrity of visuo-vestibular interaction in the brain of BVF patients. Galvanic vestibular stimulation (GVS) stimulates largely vestibular afferents but may also influence vestibular hair cells (Gensberger et al., 2016). Therefore, we used galvanic vestibular stimulation (GVS) in the fMRI scanner to test the excitability of the vestibular processing brain regions in order to investigate their responsivity once an adequate vestibular stimulus is provided. We hypothesized that this method excites visual and vestibular cortex regions in BVF better than caloric stimulation.

GVS offers the opportunity to stimulate the vestibular afferents without moving the head (Fitzpatrick and Day, 2004; Tax et al., 2013). Perceptible GVS applied to an upright subject induces postural sway towards the side of the anodal electrode with good test-retest reliability by modulating the firing rate of vestibular nerves (Tax et al., 2013). GVS has been experimentally used over the last decades not only to study behavioral responses but also brain regions' activity in response to vestibular stimulation, largely using fMRI (Bense et al., 2001; Cyran et al., 2016; Lobel et al., 1998; Stephan et al., 2005). To elucidate the specificity of vestibular-evoked brain activity we tested different perceptible stimulus intensities in a parametric design (stimulus response function, SRF) in this study. Since individual motion perception thresholds and subjective ratings differed between subjects, we used threshold-related stimulus intensities to compare similar motion perceptions rather than similar physical intensities. Moreover, GVS-evoked activity of areas with group-related differences was correlated with behavioral (vestibular) and psychophysical covariates.

On a behavioral level, perceptible GVS evokes sensation of body rotation (Fitzpatrick et al., 2002), it deviates the subjective visual vertical (Volkening et al., 2014) and it changes planned trajectories during walking (Fitzpatrick et al., 1999). Stimulation intensity is crucial but currents of 2 mA seems to reliably elicit vestibular motion perception while stimulus duration seems to have no effect on the perception intensity (Ertl et al., 2018).

In contrast, imperceptible low intensity GVS (< 0.5 mA) has been used to enhance attenuated vestibular signals in BVF patients. This is thought to be accomplished by stochastic resonance (Moss et al., 2004) in which a weak (vestibular) non-linear signal can be facilitated by adding some concurring interfering signal, i.e. white noise (Collins et al., 1995), which lowers the system's detection threshold. This signal facilitation operates best with weak subthreshold stimuli (Wuehr et al., 2018), about 0.1–0.5 mA (Goel et al., 2015). White noise (noisy GVS, nGVS) stimulation improved body balance in BVF patients during standing with the eyes closed (Iwasaki et al., 2014) and dynamic walking, particularly during slow walking (Wuehr et al., 2016b). nGVS facilitates vestibulo-spinal reflexes by lowering detection thresholds (Wuehr et al., 2018). It also improves postural stability in young (Goel et al., 2015) and elderly healthy persons which - when applied with prolonged stimulation duration - continues several hours after stimulus cessation implying neural plasticity in the vestibular system (Fujimoto et al., 2016). This sustained effect has also been shown for nGVS in BVF patients (Fujimoto et al., 2018). nGVS also seems to enhance information transfer in the central nervous system; i.e. it improves postural stability in patients with Parkinson's disease (Pal et al., 2009; Samoudi et al., 2015). Therefore, we also investigated the effects of nGVS on brain activity to investigate whether group differences in the elicited brain activity might account for the reported balance improvement.

2. Methods

Twenty-six patients with BVF (mean age 62.69 years ± 8.5 (std), 42.3% female) were enrolled in this study which was approved by the Ethics Committee of the University of Luebeck. BVF patients were enrolled from the University Centre for Vertigo and Balance Disorders. Twenty-seven age-matched healthy subjects served as controls [mean age 62.26 years ± 11.8 (std), 48.1% female]. Each participant provided informed oral and written consent in accordance with the Declaration of Helsinki.

All patients complained about dizziness, gait unsteadiness and oscillopsia during locomotion and head movements. All participants underwent neurological, neuro-ophthalmological, and neuro-otological examinations (caloric irrigation, quantitative head impulse test, subjective visual vertical). All participants were right-handed and had normal or corrected-to-normal vision. BVF patients and controls were on no regular medication known to affect central nervous system processing. None of the patients took any antivertiginous medication during the examination day.

Patients were diagnosed to have BVF based on clinical examinations by experienced neuro-otologist of the University Centre for Vertigo and Balance Disorders in Lübeck and electrophysiological recordings [bithermal cold (27°) and warm (44°) caloric irrigation, quantitative head impulse test (qHIT)]. Inclusion criteria for BVF were the following: (1) clinical assessment of a bilaterally pathologic HIT (Jorns-Haderli et al., 2007), (2) bilaterally reduced gain of the horizontal VOR (< 0.7) assessed by video-HIT (Helmchen et al., 2017; Machner et al., 2013), (3) bilateral caloric hyporesponsiveness (mean peak slow phase velocity (SPV) of < 5°/s on both sides), and (4) normal cranial magnetic resonance imaging. All patients met the criteria of BVF recently revised by a consensus group of the Barany Society (Strupp et al., 2017). Patients with depression, dementia, hearing deficits and those with additional evidence for autoimmune and paraneoplastic diseases were

excluded from the study. Pure tone audiometry showed normal hearing thresholds except for the two patients with unilateral Meniere's disease. General cognitive impairment was evaluated by the Montreal Cognitive Assessment test (MoCA). Participants were scored by neuro-otological examinations using the Clinical Vestibular Score (CVS) (Helmchen et al., 2009) and subjectively rated their level of disease-related impairment by the Dizziness Handicap Inventory score (DHI), and the Vertigo Symptom Scale (VSS) (Tschan et al., 2010). In these scores larger values indicate increased vestibular induced subjective disability (DHI, VSS) or objective impairment (CVS). The most common etiology of BVF was idiopathic BVF (n = 17) and antibiotic ototoxicity (n = 4), followed by sequential vestibular neuritis (n = 2), Meniere's disease (n = 2), and vestibular schwannoma (n = 1). All of the patients suffered from BVF for at least one year before they participated in the study. Apart from clinical signs of BVF and ataxia of stance and gait there were no other abnormal neurological signs. None of the healthy control participants had abnormal vestibular functions on clinical and quantitative recordings at the time of enrollment and recording.

Eye and head movements were recorded by the EyeSeeCam® HIT System (Autronics, Hamburg, Germany) at a sampling rate of 220 Hz. For further details see (Gottlich et al., 2016; Helmchen et al., 2017; Sprenger et al., 2014). In the MRI eye fixation and eye movements were monitored using a video based eyetracker (Eyelink 1000 Plus, 1000 Hz sampling rate, SR Research Ltd., Ottawa, ON/Ca). Horizontal and vertical eye positions were analyzed offline using Matlab® (R2017b, The Mathworks Inc., Natick, MA, USA). This was used to control fixation and to rule out eye movements as a potential covariate influencing brain activity.

2.1. Galvanic vestibular stimulation (GVS)

Bilateral bipolar GVS was applied by a current stimulator (DS5 model, Digitimer Ltd., U.K.) at both mastoid bones using contact electrodes (E224N-MR-HSR-500, EasyCap GmbH, Herrsching/Germany). This stimulator has also been used and approved in other centres and studies, e.g. (Cai et al., 2018; Cyran et al., 2016). Individual sensory (vestibular) thresholds were obtained by applying 10 s 1 Hz alternating stimulation, i.e. low frequency alternating current that passed between the two mastoid electrodes. The ramp stimulus profile hampered sharp transients at stimulus onset and offset (ramp onset and offset of 100 ms duration) with a stimulation plateau of 300 ms leading to perceived head and body tilt. Threshold testing started with an above threshold current (usually 1 mA). Subsequently, the stimulus intensity was decreased gradually in steps of 0.05 mA until the subject reported no vestibular sensations anymore. Then the procedure started again from a low threshold (0.20 mA) gradually increasing in steps of 0.05 mA until the subject reported vestibular sensations again, i.e. a perception of body motion. The threshold was verified by varying the stimulation intensity until a stable threshold was found. All subjects indicated a medio-lateral motion direction. Previous studies have shown that thresholds obtained using perceptional responses were not different from those obtained by GVS induced quantitatively analyzed body motion (Goel et al., 2015). To exclude or at least minimize nociceptive stimulation of higher GVS the stimulation site was pre-treated with local anaesthetics prior the experiment (Anesderm® lotion).

The following four stimulation intensities were used: white noise (nGVS; frequency ranging from 0.02 to 20 Hz, with a maximum of 80% of the current at perception threshold), low (0.5 mA) and high intensity current (1.5 mA) above the perceived threshold as well as sham stimulation, which consisted of a short ramp of 100 ms with the low intensity current followed by 400 ms without stimulation (Fig. 1). This kind of stimulation induced a somatosensory and nociceptive stimulation but no vestibular perception.

With the eyes open, each GVS-stimulus was examined 12 times resulting in 3 recording sessions (duration of blocks: 12 s stimulation, 4 s rating, 10 s pause interval). The sequence of experimental stimuli was pseudo-randomized. At the end of each GVS perceived motion intensity was rated on a visual analogue scale that was displayed at the end of the MR bore. The participant had to respond after a visual rating command by moving the cursor on the display of the visual analogue scale with the right hand within 4 s using a fiberoptic joystick (TETHYX, Current Designs, Inc., Philadelphia, PA/USA). Trials with no response or a late response (after 4 s) were excluded from the behavioral analysis.

2.2. Image acquisition

Structural and functional MRI images were recorded on a Siemens 3-T scanner (Magnetom Skyra) using a standard 32-channel phase array head coil. The anatomical scan was performed with a standard T1-weighted *3D turbo gradient-echo sequence* (192 sagittal slices, TR = 1.9 s, TE = 2.44 ms, matrix = 256 + ×256 mm, flip angle = 9°, voxel size = 1 mm isotropic). Functional data were acquired applying a T2*-weighted single shot gradient echo-planar imaging (EPI) sequence sensitive to blood oxygen level dependent (BOLD) contrast. The following parameters were used: repetition time TR = 1620 ms; echo time TE = 25 ms; voxel size 2.5 × 2.5 × 2.5 mm^3; field of view 263 mm; image matrix 640 × 640; 58 axial slices; slice thickness 2.5 mm; no interslice gap; flip angle 70°; three runs of each 263 volumes; simultaneous multislice (SMS) acceleration factor: 2. In order to minimize noise, ear plugs were used. Head movements were reduced by using ear pads (Multipad ear, Pearltec Technology AG, Schlieren/CH).

2.3. Preprocessing and analysis

Preprocessing and further image analysis was performed with the SPM12 software (http://www.fil.ion.ucl.ac.uk/spm; Wellcome Trust Centre for Neuroimaging, London, UK) implemented in Matlab® 2017B (MathWorks, Natick, MA). We performed a slice timing correction, motion correction by rigid body spatial transformation to the mean functional image of each dataset (individual head motion was < 3 mm or 3°, minimum to maximum), spatial normalization to a standard template (Montreal Neurological Institute, MNI), resampling to 2.5 × 2.5 × 2.5 mm^3 and spatial smoothing (6 mm full width half maximum Gaussian kernel). Individual head motion was estimated by the six realignment parameters, i.e. three rotational and three translational movements with respect to the first image in the EPI series. Functional MRI time series were modeled using a general linear model (GLM). The GLM included regressors for the start of every type of stimulation trial convolved with the canonical hemodynamic response function of SPM12. The six motion parameters were used as covariates in the GLM.

2.4. Analysis

At first level, using whole brain analysis we contrasted brain activity during GVS trials (nGVS, lowGVS, highGVS) against SHAM stimulation (high level baseline) to exclude unspecific nociceptive stimulation. We used a flexible factorial design modelling the factors SUBJECT, GROUP, STIMULATION (intensity) and the interaction GROUP x STIMULATION (intensity) (Gläscher, 2008). To investigate the role of the perceived threshold of GVS on brain activity we additionally used this threshold as covariate within this flexible factorial design.

Differences in brain activity between patients and controls were investigated using a 2 × 3 flexible factorial design with the factor 'GROUP' (2 levels: patients, controls) and the factor 'STIMULATION'(3 levels: nGVS, lowGVS, highGVS). Statistical images were assessed for cluster-wise significance using a cluster defining threshold of p = .05 with family wise error (FWE) correction for multiple testing. Activations were anatomically localized with the Automated Anatomical Labeling (AAL, (Tzourio-Mazoyer et al., 2002)) and cytoarchitectonic probability maps (Eickhoff et al., 2007; Eickhoff et al., 2005). Regions of interest (ROI taken from both sides) were defined by

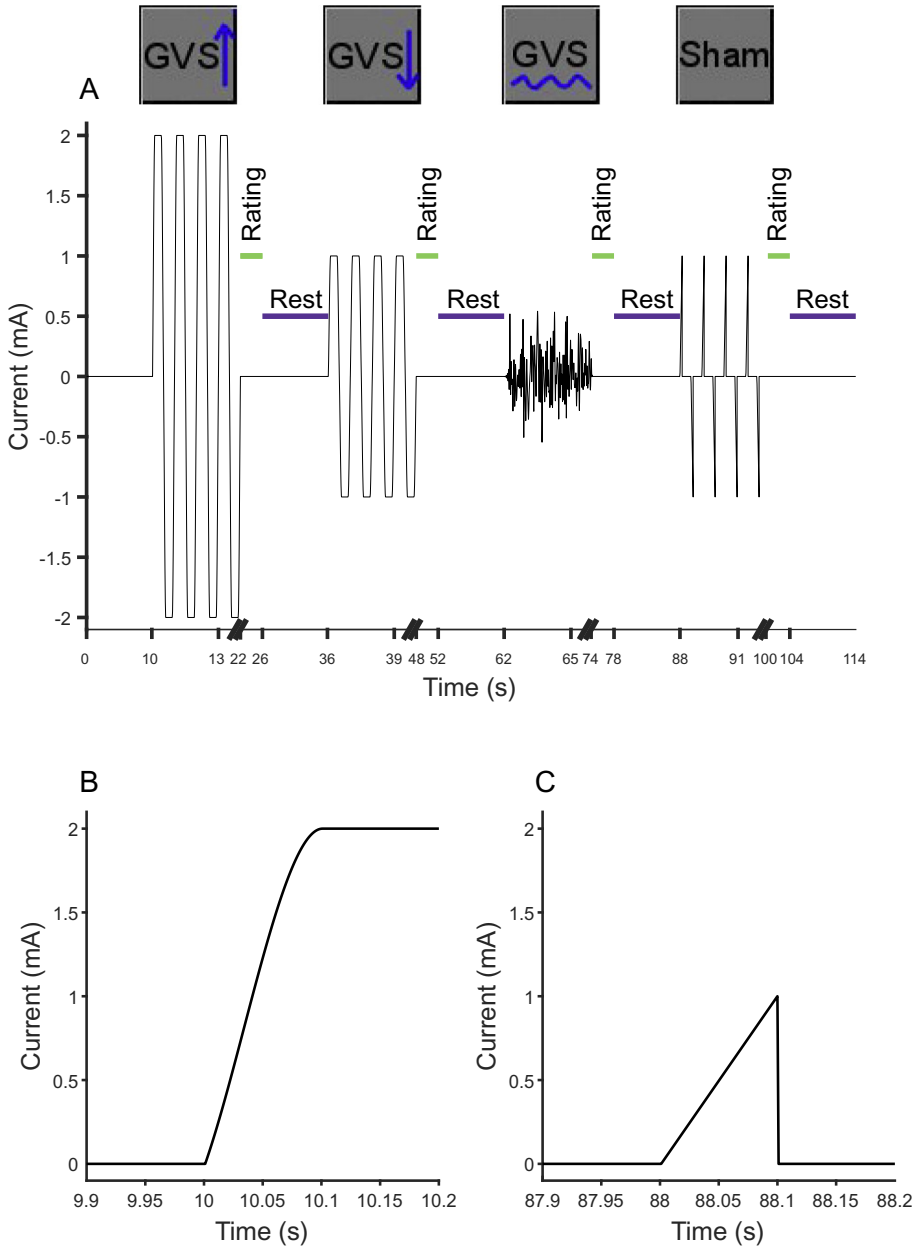

Fig. 1. (A) Schematic drawing of the four stimulation types used in the study with a low stimulation of 1.0 mA and a high stimulation 2.0 mA (12 s), which was followed by a rating (max. 4 s) and a rest period (10 s). (B) and (C) show a magnified view of ramps shown in (A). (B) In order to minimize cutaneous stimulation in low and high GVS stimulation a 100 ms smooth ramp was used instead of sharp transients. After a plateau of 300 ms a ramp offset was used to change the stimulation side. (C) For sham stimulation, a linear ramp stimulation (100 ms) was used which induced no vestibular perception.

using SPM Anatomy Toolbox [(Version 2.2b, (Eickhoff et al., 2005)].

2.5. Statistical analysis

Statistical analyses were performed with SPSS (22.0.0.2; IBM Corp., Somer NY), with ANOVAs for comparison of groups and conditions (three stimulation contrasts), post-hoc *t*-tests and Pearson correlation analyses with behavioral and disease parameters. In some comparisons, sphericity requirement was violated. Therefore, we report *p*-values with Greenhouse-Geisser correction but report degrees of freedom (df) uncorrected in order to show the factorial analysis design. Statistical comparisons were performed parametric unless stated otherwise.

Multi-factorial ANOVA with the above mentioned factors were performed. Significance levels of post-hoc tests were Bonferroni corrected for multiple testing. Statistical differences were regarded as significant for values $p < .05$ and Bonferroni-corrected for multiple comparisons (Chumbley et al., 2010; Chumbley and Friston, 2009). Error bars indicate mean values (M) and standard error of mean (SE) unless otherwise stated. Correlation analyses were performed using Spearman-Rho coefficient unless otherwise stated.

3. Results

3.1. Psychophysics

3.1.1. Clinical scores

Subjective disease-related impairment for the Dizziness Handicap Inventory (DHI) revealed on average 39.35 ± 2.48, and 24.38 ± 4.04 for the Vertigo Symptom Scale (VSS). The Clinical Vestibular Score (CVS) revealed on average 10.04 ± 0.78 in BVF patients (Gottlich

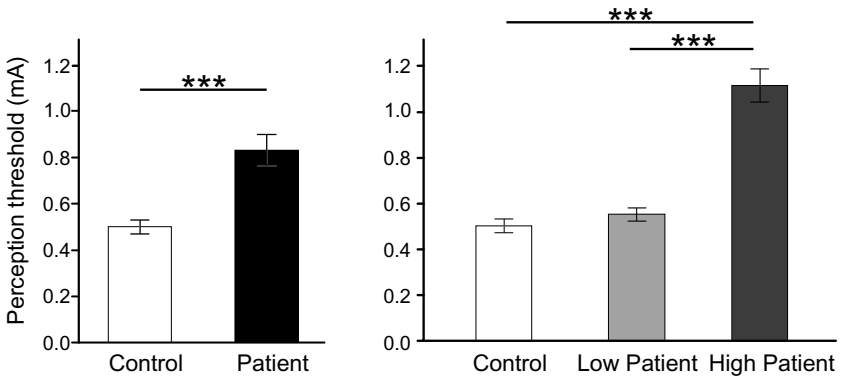

Fig. 2. Mean perception thresholds of GVS are shown for BVF patients and healthy participants (A). Patients had a significantly higher threshold than healthy controls ($t(51) = -4.482$ ($p < .001$). Fig. 2B shows a split half analysis (cutoff: 0.83 mA) comparing the low with the high threshold patient group (each $n = 13$). Error bars indicate standard error of mean. * ≤0.05; *** ≤0.001.

et al., 2014; Helmchen et al., 2014). Mean disease duration was 7.37 ± 6.47 (range 1–32.3 years). There was no correlation of any of these scores with disease duration (always $p > .2$) or the VOR gain.

3.1.2. Perception threshold

The perception threshold of GVS was higher in BVF patients (0.83 mA ± 0.06) compared to controls (0.5 mA ± 0.03) ($t(51) = -4.45$ ($p < .001$) (Fig. 2A). Most of the patients were close to a narrow threshold of 0.5 mA but several other patients had a markedly higher perception threshold above 0.83 mA with a large variability; therefore we performed a split half analysis (cutoff: 0.75 mA) comparing a low (normal) threshold patient group ($n = 13$, mean threshold = 0.55 ± 0.03 mA) with a high threshold patient group (mean = 1.11 ± 0.07 mA; n = 13) (Fig. 2B) which both differed significant from each other and the control group ($F(2,50) = 62.94$; post-hoc t-tests each $p < .001$). Three of the patients with a higher perception threshold had a history of vestibular nerve disease (e.g. vestibular neuritis, acoustic neuroma) sparing the vestibular end organ.

Rating of perceived motion was significantly different between the four stimuli (Fig. 3). Patients rated GVS higher (39.36 ± 2.6) than healthy control subjects (33.23 ± 2.6) ($F(1,51) = 5.47$, $p < .03$), particularly the rating of perceived sway of patients was higher during highGVS, while the trend towards higher ratings in patients with the other stimuli (pairwise comparison) just failed significance. Participants reported no pain during GVS. Overall, ratings of the perceived intensities of the different galvanic stimuli were not related to the perceived threshold (correlation coefficients always $p > .155$; Fig. 3, see magnified box on the right), i.e. individual thresholds do not allow to predict ratings of individual perceived GVS.

3.2. Vestibulo-ocular reflex

The mean gain of the patients' horizontal vestibulo-ocular reflex (VOR), tested by quantitative head impulse test, was severely reduced (right: 0.275 ± 0.04; left: 0.271 ± 0.04), compared with healthy controls (right: 0.97 ± 0.03; left: 0.99 ± 0.02). Subjective visual vertical did not show pathological tilts (> 2.5°) and did not differ between patients and controls, neither for the dynamic nor the static SVV.

3.3. Imaging results

3.3.1. Stimulus intensity related brain activity

Using whole brain analysis, there was a main effect for STIMULUS INTENSITY (nGVS, lowGVS, highGVS) in both patients and healthy control subjects (FWE corrected $p < .05$) (Fig. 4), i.e. activation increased with stimulus intensity in several multisensory areas including those known to be associated with vestibular processing, e.g. insula, posterior operculum, superior temporal gyrus, inferior parietal lobe, visual cortex, cingulate cortex, and cerebellum (Table 1). Note that this is GVS-evoked activity exceeding SHAM-related activity (baseline contrast). However, stimulus intensity coding differed between regions (Fig. 5; Table 2), e.g. activity in superior temporal gyrus (STG),

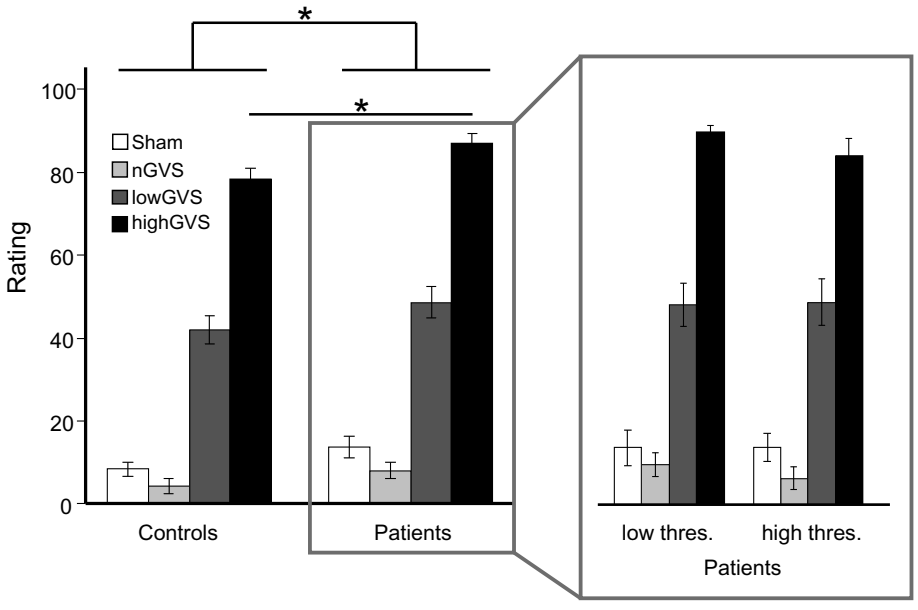

Fig. 3. Ratings of the four different galvanic vestibular stimuli (Sham, nGVS, lowGVS, highGVS) are shown for healthy participants and BVF patients. Patients showed higher ratings, particularly in the highGVS condition (* ≤0.05). The magnified view on the patient group reveals that there is no difference in rating of perceived motion perception between the low (n = 13) and high (n = 13) threshold subgroups of patients.

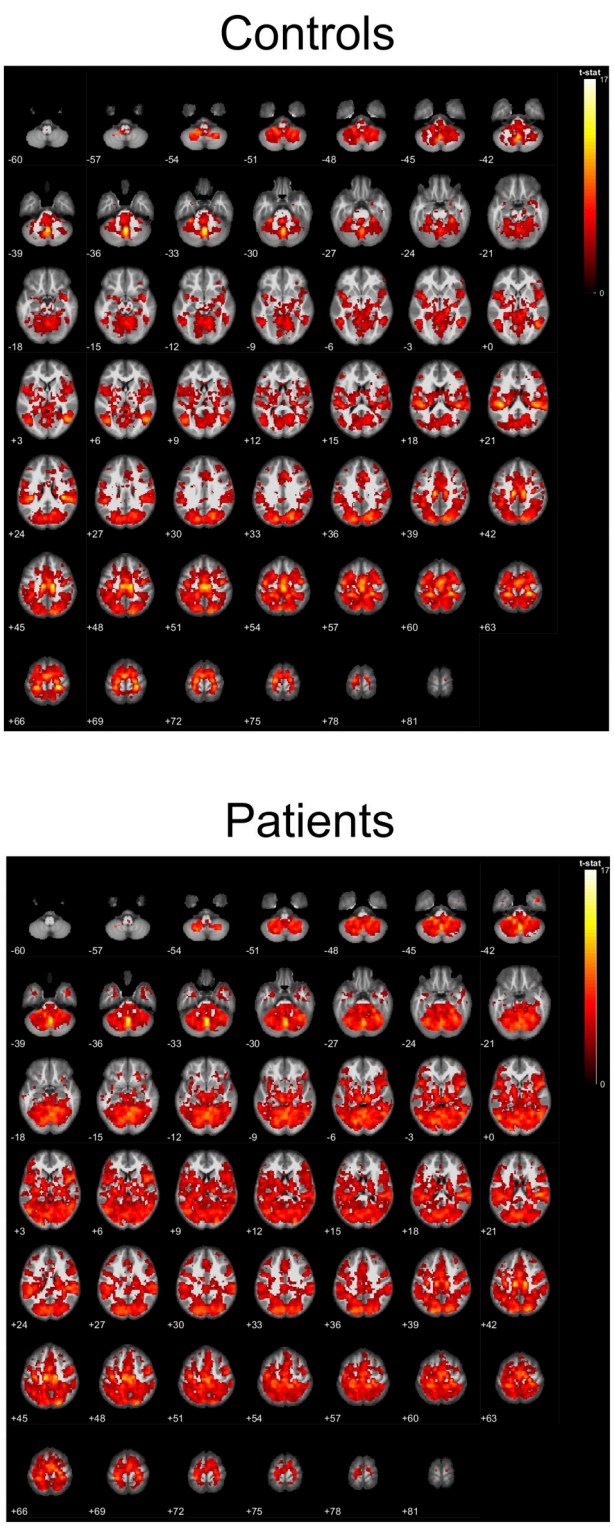

Fig. 4. Main effect of brain activity for the contrast GVS > sham are shown for healthy controls (left) and BVF patients (right). Generally, there was a trend towards higher activity in patients. Statistical images were assessed for whole brain analysis with FWE-correction ($p = .05$). T-values are indicated on the bar. Activated brain regions with anatomical labelling and MNI coordinates are listed in Table 1.

operculum (OP1,2,4), insula, and vermis increased significantly with stimulus intensity (correlation coefficient up to $r = 0.61$ in OP2; $p < .001$) while there was no stimulus intensity coding, e.g. in hippocampus and the intraparietal sulcus. Correlation coefficients

Table 1
Brain activation (main effect) for the contrast highGVS > sham stimulation for healthy control subjects and BVF patients (FDR and FWE corrected p < .05).

Main effect activation by highGVS > sham stimulation (healthy control) FDR and FWE corrected $p < 0,05$

Cluster	Brain region	Cluster size	x	y	z	t value
Cluster 1	Postcentral gyrus R	14,619	26	−35	68	16.23
	Insula R		38	−30	23	15.58
	Vermis R		1	−60	−35	15.05
Cluster 2	Temporal mid R	478	48	−65	3	11.47
	Temporal inf R		46	−42	−15	6.32
	Temporal inf R		56	−52	−13	6.30
Cluster 3	Temporal mid L	579	−42	−67	8	10.92
	Temporal inf L		−50	−55	−8	7.61
	Temporal inf L		−55	−62	−10	6.76
Cluster 4	Cingulate mid R	121	13	16	35	8.89
	Cingulate ant R		13	16	25	5.29
Cluster 5	Insula L	370	−40	3	−5	8.29
	Precentral gyrus L		−57	3	20	7,99
	Rolandic operculum L		−47	8	3	6.94
Cluster 6	Insula R	55	41	1	−15	7.96
Cluster 7	Pallidum L	158	−25	−17	3	7.25
	Putamen L		−30	−20	10	6.83
	Putamen L		−27	3	8	6.32
Cluster 8	Insula R	350	46	1	3	7.13
	Frontal inf operculum R		53	8	18	7.03
	Rolandic operculum R		38	−5	15	6.56
Cluster 9	Calcarina R	33	28	−50	8	7.13
Cluster 10	Hippocampus L	50	−27	−37	5	6.90
Cluster 11	Cuneus L	23	−20	−57	20	6.83
Cluster 12	Frontal mid 2 R	35	46	38	20	6.02
Cluster 13	Frontal sup med L	18	−7	26	40	5.44

Main effect activation by highGVS > sham stimulation (patient) FDR and FWE corrected p < 0,05

Cluster	Brain region	Cluster size	x	y	z	t value
Cluster 1	Vermis R	31,571	1	−60	−35	14.47
	Cingulate mid L		−12	−22	45	13.44
	Cingulate mid R		13	−17	43	11.92
Cluster 2	Cingulate post R	54	3	−37	8	7.40
Cluster 3	Temporal pole mid R	40	43	11	−43	7.35
	Temporal inf R		38	3	−43	6.74
Cluster 4	Pallidum R	30	16	6	0	6.74
Cluster 5	Parahippocampal L	26	−30	1	−30	5.74
Cluster 6	Parahippocampal R	18	26	3	−33	5.63

indicating larger activity during highGVS vs. lowGVS are displayed in Table 2. In contrast to perceptible GVS, nGVS did not elicit significant activations (FWE $p < .05$).

3.3.2. Group differences

There was a general trend for higher GVS-related activation in the patients'brain compared to controls (Fig. 4) which was significant in the whole brain analysis for the visual cortex, specifically area hOC3v (Rottschy et al., 2007) bilaterally (Fig. 6, FWE corr. p < .05; FDR-corr. p < .05, Table 3) and the middle temporal gyrus. According to the cytoarchitectonic probability maps (SPM toolbox), the clusters were found in bilateral visual cortex, i.e. in the left occipital gyrus with a 30% probability of hOc3v [V3v], 43% in hOc4p and 25% in hOc4v [V4v] and right calcarine gyrus with a 56% probability of hOc1 [V1]. The left fusiform gyrus activation was assigned with a 57% probability to area of hOc4v [V4v], and 20% to hOc3v [V3v] and left middle temporal gyrus with a 32% probability assignment to area TE3.

Using small volume correction (FWE p < .001 uncorrected), there

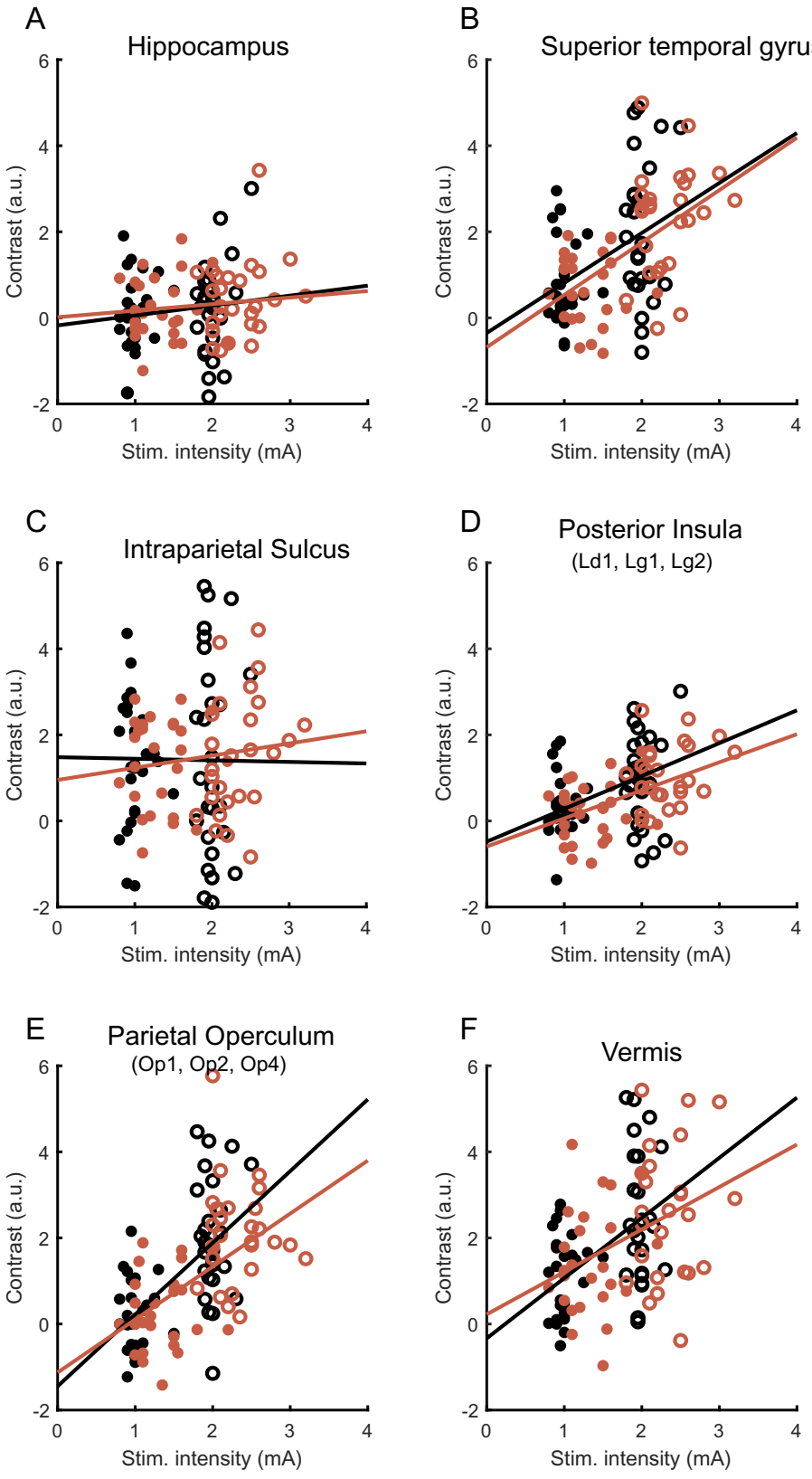

Fig. 5. Stimulus intensity-dependent neural activity in distinct cerebral regions of interest known to be involved in vestibular processing is displayed (lowGVS = filled circles; highGVS = open circles). The median contrast values for each stimulus intensity [mA] (lowGVS, highGVS) were depicted from the regions of interest (left and right side) according to the SPM Anatomical Toolbox for healthy control subjects (black) and BVF patients (red). Activity in superior temporal gyrus (STG, B), operculum (OP1,2,4; E), insula (D), and vermis (F) increased significantly with stimulus intensity while there was no stimulus intensity coding, e.g. in hippocampus (A) and intraparietal sulcus (C, see Table 2).

was additional larger activity in the middle (MTG) and superior temporal gyrus (STG) of the patients, at the lower rim of the inferior parietal lobule (IPL), the left middle frontal gyrus and the right head of the caudate nucleus. According to cytoarchitectonic probability maps the clusters were assigned to the right superior temporal gyrus, with a 47% probability to the inferior parietal lobule (IPL_PF) and a 34% to TE3, and to the left middle temporal gyrus with 13% probability to area TE3. There was no interaction of STIMULATION x GROUP ($p < .05$). The GVS-evoked brain activity in patients (see Table 3) increased with larger subjective dizziness-related handicap (Fig. 7): t-contrast values of

Table 2
Correlations of median contrast values (highGVS vs. Sham, lowGVS vs. Sham) with individual stimulation intensity (mA) for regions of interest, derived from Anatomy Toolbox Version 2.2b (Eickhoff et al., 2007). Depicted values are Spearman-Rho correlation coefficients and corresponding p-values.

Region specific intensity coding of GVS (high > lowGVS)			
	region	correlation coefficient (r)	p-Value
Patient	Hippocampus	0.15	0.287
	Thalamus	0.37	**0.008**
	V1	0.34	**0.01**
	V3	0.35	**0.01**
	V5	0.37	**0.001**
	Cerebellum (hemisphere)	0.27	**0.04**
	IPL/STG	0.54	**0.001**
	IPS	0.11	0.42
	Insula (LdLg12)	0.47	**0.001**
	Vermis	0.36	**0.009**
	OP (1,2,4)	0.61	**0.001**
Control	Hippocampus	0.15	0.288
	Thalamus	0.16	0.254
	V1	0.16	0.246
	V3	0.17	0.209
	V5	0.25	0.068
	Cerebellum (hemisphere)	0.16	0.245
	IPL/STG	0.31	0.024
	IPS	−0.07	0.245
	Insula (LdLg12)	0.22	0.104
	Vermis	0.39	**0.004**
	OP (1,2,4)	0.54	**0.001**

highGVS vs. sham stimulation correlated with the DHI in STG (r = 0.43; p = .029) and with the VSS and CVS in the visual cortex (V3; r = 0.47; p = .015 and r = 0.40; p = .049, respectively). The contrast values in these regions did not correlate with the extent of the vestibular impairment (gain of the VOR, SVV) or disease duration (always $p > .05$).

Remember, we perceptionally matched galvanic vestibular stimuli rather than physical current intensity due to disease related changes of perception thresholds. To investigate the role of the perceived threshold of GVS on brain activity we finally used this threshold as covariate within our flexible factorial design. The significant group differences in the visual cortex (hOc3v/hOc4p) were unchanged [FWE and FDR corrected p < .05; MNI: −25 -92 0; t-value: 7.17; MNI:8–97 5; t-value: 6.62; MNI:-20–77 -5; t-value: 5.72; MNI: 38–85 3, t-value: 5.56]; i.e. they were independent of the differences in stimulus intensity used. The bilateral temporal cortex activity (STG) just failed significance in this analysis.

There was no significant (FDR < 0.05 corr.) difference in activation when patients with normal vestibular perception thresholds (n = 13) were compared with those with higher thresholds (n = 13) (low vs. high threshold patient subgroups). Using the individual perception threshold as covariate there was also no significant interaction group x stimulus intensity.

4. Discussion

Perceptible (low, high GVS) but not imperceptible (nGVS) galvanic vestibular stimulation evoked a pronounced brain activity in BVF patients that differed between groups in early visual, middle frontal, and

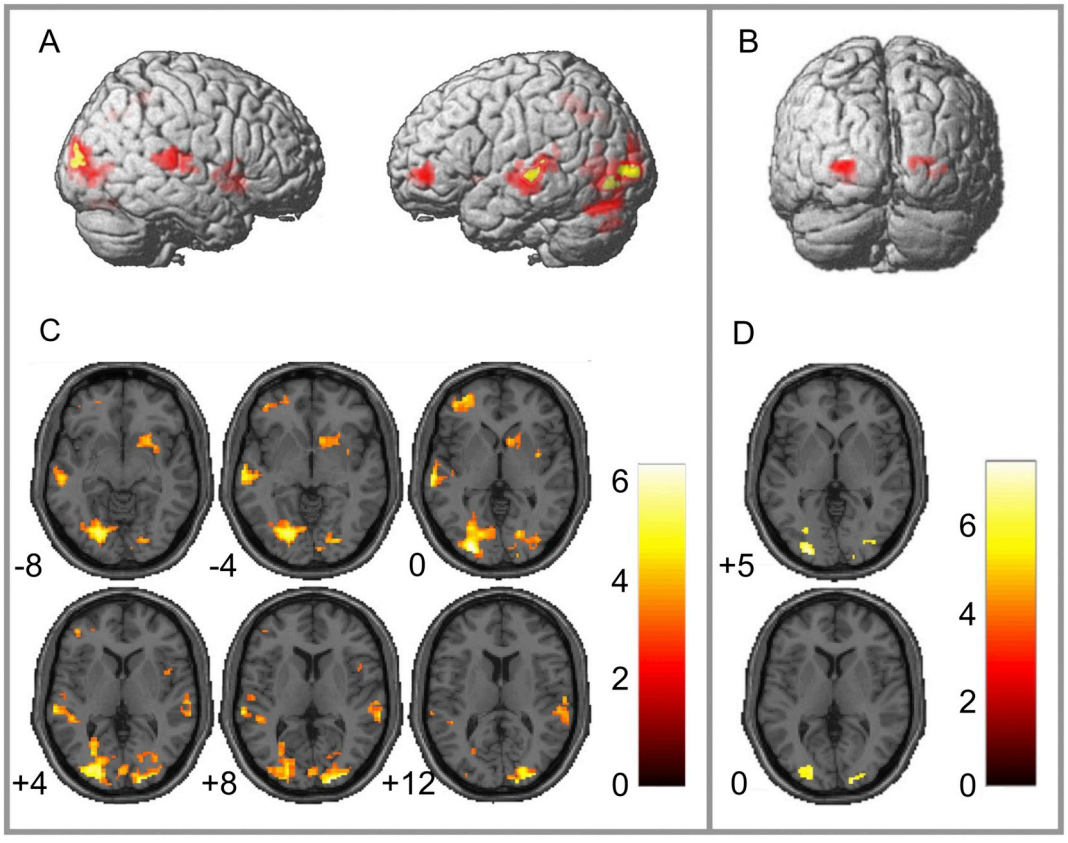

Fig. 6. Group comparison (t-contrasts) of the brain activity of patients and healthy control subjects in response to galvanic vestibular stimulation (highGVS > sham) shows stronger inferior occipital and superior temporal lobule activation in patients in 3D surface display (A) and axial (C) slices. Using the individual threshold as a covariate in the analysis (s.methods) the occipital activation remains stable (B, D), i.e. it is independent of the individual threshold [whole brain analysis: yellow = $p < .05$ FWE corrected; red ≤0.001 FWE uncorrected].

Table 3
T-contrasts for the group comparison patients vs. healthy controls (patients > healthy control) are shown (whole brain analysis, FWE corrected $p < .05$, see yellow activations in Fig. 6A). Clusters are assigned to brain regions by using the cytoarchitectonic probability maps (SPM toolbox; n.a. = not assigned). Using small volume correction (FWE unc. $p < .001$) revealed superior temporal gyrus activations bilaterally, caudate and middle frontal gyrus. There was no significant activation in healthy control subjects larger than in patients.

t-Contrasts for the group comparison patient > healthy control (whole brain analysis)

Region		Cluster size	x	y	z	$p_{\text{-FWE-corr}}$	t value
hOc3v/hOc4p	Inferior occipital gyrus	60	−25	−92	0	0.001	6.32
hOc1	Calcarine gyrus	28	18	−97	8	0.001	6.08
hOc1	Middle temporal gyrus	18	−62	−22	−3	0.001	6.04
hOc4v	Fusiform gyrus	30	−22	−75	−8	0.004	5.61
Small volume corrections							
STG/MTG	Superior/middle temporal gyrus	68	−62	−25	−3	0.006	5.45
IPL_PF/STG	Superior temporal gyrus	20	66	−35	−10	0.026	4.83
n.a.	Middle frontal gyrus	73	−42	46	−3	0.029	4.48
n.a.	Caudate region	61	11	13	3	0.022	4.54

t-Contrasts for the group comparison patient < healthy control (whole brain analysis)

None

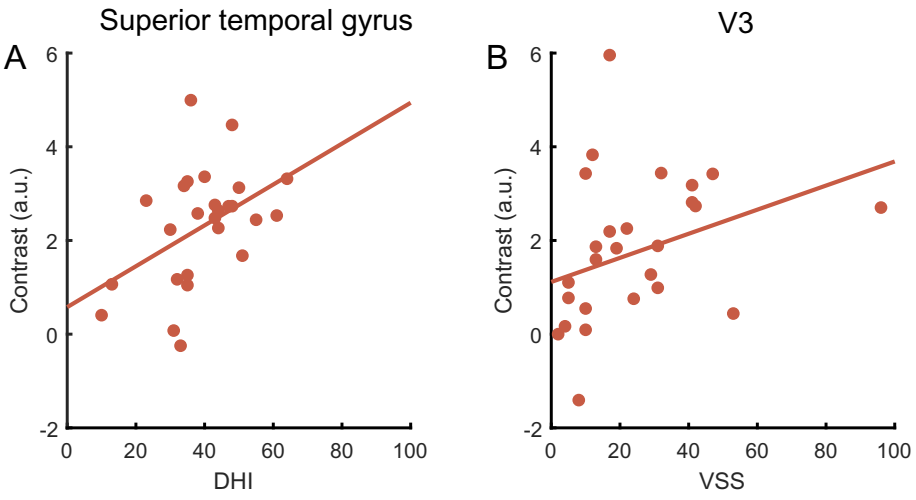

Fig. 7. Relation of contrast estimates in regions with group-related increased GVS evoked brain activity in patients (significant group differences, see Table 3), i.e. superior temporal gyrus in (A) and visual cortex (V3 in B), and clinical scores [the Dizziness Handicap Inventory score (DHI), Vertigo Symptom Scale (VSS)]. Activity in these regions was associated with larger subjective dizziness-related handicap.

temporal cortex areas. Despite chronic sensory deafferentation, the brain responds to vestibular stimuli very similar compared to healthy subjects (e.g. with parallel stimulus response functions). This sheds light on the potential application of peripheral vestibular implants or mastoid galvanic stimulators in BVF patients.

A major group difference was the increased GVS-evoked activity in the visual cortex in BVF patients. Visual cortex activity is known to be altered in response to sensory, i.e. visual (Ahmad et al., 2017; Deutschlander et al., 2008; Roberts et al., 2017; Roberts et al., 2018) and proprioceptive (Cutfield et al., 2014) stimuli in patients with uni- and bilateral vestibular failure but (galvanic) vestibular stimulation in BVF had not been studied before.

4.1. Visual sensitivity in BVF

A leading clinical problem of vestibular failure patients is head- and locomotion-related oscillopsia since the vestibulo-ocular reflex cannot stabilize gaze during head movements any more. Mechanisms of adaptation are the increase of perception thresholds for visual motion detection and the increase of tolerance to retinal slip (Shallo-Hoffmann and Bronstein, 2003). Neurophysiologically, neural activity in the visual cortex of BVF during visual stimuli is changed (Arshad et al., 2014; Deutschlander et al., 2008; Kalla et al., 2011). Downregulation of the primary visual cortex activity may play an important role in the suppression of visuo-vestibular symptoms (Brandt et al., 1998; Roberts et al., 2017).

On the other hand, increased visual sensitivity is a known competing mechanism of sensory re-weighting in the visual cortex to substitute for bilaterally deficient vestibular inputs. This enhancement of visual cortex activity in BVF (Dieterich et al., 2007) needs to be balanced as it should not provoke visual vertigo (Cousins et al., 2017) or the perception of oscillopsia. In fact, visual dependence of BVF patients is a known predictor for poorer recovery (Cousins et al., 2014).

4.2. Reciprocal visual-vestibular interaction

In order to dissociate self-motion from object motion, reciprocal inhibitory interaction between cortical areas responding to visual and vestibular stimuli is postulated which helps to modulate the excitability in the case of non-congruent, i.e. conflicting information of spatial orientation. According to the hypothesis of reciprocal inhibition (Brandt et al., 1998), the excitability of areas involved in processing vestibular signals (e.g. retroinsular cortex) is suppressed by visual motion stimuli. In turn, the perception of involuntary retinal slip due to vestibular stimulation is reduced by attenuation of the excitability of the visual cortex. This insures self-motion sensation during body displacement

and visual motion perception (Ventre-Dominey, 2014). When visual stimuli are presented in combination with vestibular caloric stimulation early visual cortex excitability is changed depending on the fact if both sensory cues are congruent or in conflict (Roberts et al., 2017).

In contrast, our BVF patients showed larger activity in bilateral visual cortex during fixation with perceptible GVS, involving visual cortex areas V1 (hOc1) to largely V3 (hOc3v and hOc4v). Area V3 has an intermediate position in the visual processing hierarchical structure since it is strongly connected to primary visual cortex (V1, V2)(Helfrich et al., 2013) but also to the motion sensitive area MT/V5 and V6 (Galletti et al., 2001).

There are several conceivable explanations for the higher visual cortex activity in BVF patients: First, GVS activates multisensory neurons in the visual cortex stronger than in controls due to chronic sensory (vestibular) deprivation, e.g. by sensory "re-weighting" (Angelaki et al., 2009; Fetsch et al., 2009). The reduced cortical excitability in the visual cortex of BVF patients to visual and magnetic stimuli (Ahmad et al., 2017) may be associated with increased vestibular excitability due to crossmodal plastic reorganization. However, multireceptive cells were found in area MSTd of the macaque monkey but not in the early visual cortex (Chen et al., 2008). Second, it could be another sign of visual substitution of bilateral vestibular failure (Dieterich et al., 2007) but in contrast to the latter study, we provided vestibular but not visual stimuli. Third, reciprocal inhibitory cortical visual-vestibular interaction is probably impaired in our BVF patients as GVS does not inhibit (deactivate) early visual cortex activity as in healthy subjects.

4.3. Vestibular stimulation in BVF

In contrast to a previous PET ($H_2{}^{15}O$) study (Bense et al., 2004b), we found strong but indistinguishable cortical responses to GVS in parieto-insular and temporal regions of both groups (see main effects of high > lowGVS contrasting sham for each group separately). There was even a trend to more excitability in BVF patients. This may be due to the mechanisms of action. While caloric irrigation stimulates the semicircular canals at the end organ, GVS activates vestibular afferents (Tax et al., 2013).

Our data extend the study by Bense and coworkers (Bense et al., 2004b) in that the increased visual cortex excitability to GVS in our patients could reflect the proposed attenuated inhibitory visual-vestibular interaction in BVF: normal (indistinguishable from healthy controls) excitability in vestibular processing cortical regions (e.g. OP2, insula, cingulate) elicited activation of early visual cortex areas instead of deactivation. However, it is not related to a reduced excitability of cortical vestibular regions (e.g. OP2, insula, IPL, STG) but possibly subject to an inherent deficit in functional connectivity between multisensory early visual and vestibular cortical regions. It remains an open question for future studies whether application of portable mastoid devices with continuous GVS may reverse this abnormal visual-vestibular interaction to a normal inhibitory level.

BVF patients showed increased activity in superior temporal gyrus (STG) bilaterally, which is known to be involved in vestibular processing (Cian et al., 2014; Cutfield et al., 2014; Dieterich and Brandt, 2008; Gottlich et al., 2014; Helmchen et al., 2014; Karim et al., 2013; Kim et al., 2018; Ruhl et al., 2018; Zu Eulenburg et al., 2011; zu Eulenburg et al., 2013). These activations were at the lower rim of the supramarginal gyrus of the inferior parietal lobe but rostral to opercular area OP2, the human homologue to the parietoinsular vestibular cortex (PIVC) in macaque monkeys (Zu Eulenburg et al., 2011). OP2 has been identified as a crucial network hub of functional connectivity during conflicting visual-vestibular motion (Ruhl et al., 2018).

The greater activity in STG of patients could be due to cortical sensitization by vestibular deprivation in BVF. However, in this case one should have also expected higher activity in OP2.

4.4. Relation of perceived motion threshold and visual and temporal cortical activity

Since there was a larger variability of perceived motion detection thresholds in our BVF patients we divided them into two groups of high and low (indistinguishable from the controls) thresholds. High threshold patients showed increased activity in the middle temporal gyrus and the temporal pole but not in the STG region where the group differences were found. In some patients vestibular nerve disease (acoustic neuroma, sequential vestibular neuritis) was probably responsible for the elevated perception threshold. The data, however, show that even with elevated motion perception thresholds there is a stronger vestibular excitability in the patients' visual and vestibular cortical areas. This is in line with the fact that the significant group differences in visual and vestibular cortex activity were not correlated with the individual perception thresholds.

4.5. Stimulus intensity coding of cortical activity (stimulus response functions)

As we anticipated differences in the motion detection thresholds in some of the BVF patients, we adapted the applied low and high galvanic stimulus intensity to the individual motion perception threshold. This assured comparisons of evoked brain activity during similar percepts rather than identical physical current intensities. Patients still turned out to have slightly higher ratings, particularly for high GVS that might account for the higher activation in STG.

We found several significant increases in neural activity with increasing stimulus intensities (high > low GVS), particularly in regions known to be involved in processing vestibular signals: parietal operculum (OP1, 2 and 4), insula, thalamus, midline cerebellum, early visual cortex (V1, V2) but also motion sensitive areas like MST/V5. These correlations were more significant in patients (Table 2) but generally there was no significant group difference. The steepness of the stimulus response function indicates the likelihood that this brain region is involved in vestibular signal processing or the perception of vestibular stimuli, respectively. As expected, we found strong correlations in OP2, insula, cerebellar vermis, and STG (bordering IPL), all of which contain multireceptive neurons responding to vestibular stimuli (Lopez and Blanke, 2011). We anticipated diverging slopes of SRF in these vestibular cortical regions with a more moderate steepness in BVF patients. Given the elevated motion perception thresholds it is remarkable that both groups have indistinguishable stimulus response functions reflected by their parallel curves. This may reflect different mechanisms underlying perception thresholds and motion intensity coding.

4.6. Imperceptible galvanic vestibular stimulation (nGVS)

One aim of this study was to identify cortical changes in activity during nGVS to provide an additional putative cortical explanation for the improved performance of BVF patients in stance (Iwasaki et al., 2014) and gait (Wuehr et al., 2016b). The common explanation for this effect is stochastic resonance (Moss et al., 2004) in which a weak (vestibular) non-linear signal can be facilitated by adding some concurring interfering signal, i.e. noise (Collins et al., 1995), which lowers the system's detection threshold. Accordingly, nGVS facilitates vestibulospinal reflexes by lowering detection thresholds (Wuehr et al., 2018). However, we did not find any significant activations during nGVS being superior to sham stimulation, nor did we find any group differences.

nGVS requires an additional weak sensory (vestibular) stimulus which should then be better discriminated, even on a cortical level. Since we did not examine nGVS with a concomitant perceptible vestibular stimulus it remains speculative and up to future studies whether balance improvement by nGVS is also caused by cortical mechanisms.

4.7. Potential clinical implications

We consider it of potentially great clinical importance that the cortical vestibular system in BVF responds to peripheral galvanic vestibular stimuli in a similar way (stimulus-response functions) than healthy controls as it might make the application of vestibular implants (Fornos et al., 2017; van de Berg et al., 2017) or portable GVS pacemakers feasible (Wilkinson et al., 2014; Wuehr et al., 2016a).

However, these applications must consider that a few multisensory integratory visual and vestibular brain regions (V1-V3, STG) showed increased responsitivity which correlated with the severity of vestibular symptoms and dizziness-related handicap in daily life suggesting a potential clinical role. It will be of great clinical interest whether vestibular stimulation via these devices can reverse the increased excitability.

The study extends previous studies by showing that clinical improvement is linked to brain function rather than restitution of peripheral vestibular function.

4.8. Limitations of the study

Even when using local anaethetics prior GVS the concomitant nociceptive stimulation remains a potential confound. Therefore, we introduced a sham stimulation without motion percept and contrasted all analyses against this baseline. Consequently, nociceptive stimulation probably does not account for the reported activation.

To rule out differences in the motion perception of the participants we matched similar percepts rather than similar physical current intensities. The early visual cortex activation remained significant even when the individual motion perception threshold is taken as a covariate, i.e. the activation was independent of the thresholds.

References

Ahmad, H., Roberts, R.E., Patel, M., Lobo, R., Seemungal, B., Arshad, Q., Bronstein, A., 2017. Downregulation of early visual cortex excitability mediates oscillopsia suppression. Neurology 89, 1179–1185.

Angelaki, D.E., Gu, Y., DeAngelis, G.C., 2009. Multisensory integration: psychophysics, neurophysiology, and computation. Curr. Opin. Neurobiol. 19, 452–458.

Arshad, Q., Nigmatullina, Y., Bronstein, A.M., 2014. Unidirectional visual motion adaptation induces reciprocal inhibition of human early visual cortex excitability. Clin. Neurophysiol. 125, 798–804.

Becker-Bense, S., Dieterich, M., Buchholz, H.G., Bartenstein, P., Schreckenberger, M., Brandt, T., 2014. The differential effects of acute right- vs. left-sided vestibular failure on brain metabolism. Brain Struct. Funct. 219, 1355–1367.

Bense, S., Stephan, T., Yousry, T.A., Brandt, T., Dieterich, M., 2001. Multisensory cortical signal increases and decreases during vestibular galvanic stimulation (fMRI). J. Neurophysiol. 85, 886–899.

Bense, S., Bartenstein, P., Lochmann, M., Schlindwein, P., Brandt, T., Dieterich, M., 2004a. Metabolic changes in vestibular and visual cortices in acute vestibular neuritis. Ann. Neurol. 56, 624–630.

Bense, S., Deutschlander, A., Stephan, T., Bartenstein, P., Schwaiger, M., Brandt, T., Dieterich, M., 2004b. Preserved visual-vestibular interaction in patients with bilateral vestibular failure. Neurology 63, 122–128.

van de Berg, R., Guinand, N., Ranieri, M., Cavuscens, S., Nguyen, T.A.K., Guyot, J.P., Lucieer, F., Starkov, D., Kingma, H., van Hoof, M., Perez-Fornos, A., 2017. The vestibular implant input interacts with residual natural function. Front. Neurol. 8.

Brandt, T., Bartenstein, P., Janek, A., Dieterich, M., 1998. Reciprocal inhibitory visual-vestibular interaction. Visual motion stimulation deactivates the parieto-insular vestibular cortex. Brain 121 (Pt 9), 1749–1758.

Cai, J., Lee, S., Ba, F., Garg, S., Kim, L.J., Liu, A., Kim, D., Wang, Z.J., McKeown, M.J., 2018. Galvanic vestibular stimulation (GVS) augments deficient Pedunculopontine nucleus (PPN) connectivity in mild Parkinson's disease: fMRI effects of different stimuli. Front. Neurosci. 12, 101.

Chen, A., Gu, Y., Takahashi, K., Angelaki, D.E., Deangelis, G.C., 2008. Clustering of self-motion selectivity and visual response properties in macaque area MSTd. J. Neurophysiol. 100, 2669–2683.

Chumbley, J.R., Friston, K.J., 2009. False discovery rate revisited: FDR and topological inference using Gaussian random fields. NeuroImage 44, 62–70.

Chumbley, J., Worsley, K., Flandin, G., Friston, K., 2010. Topological FDR for neuroimaging. NeuroImage 49, 3057–3064.

Cian, C., Barraud, P.A., Paillard, A.C., Hidot, S., Denise, P., Ventre-Dominey, J., 2014. Otolith signals contribute to inter-individual differences in the perception of gravity-centered space. Exp. Brain Res. 232, 1037–1045.

Collins, J.J., Chow, C.C., Imhoff, T.T., 1995. Stochastic resonance without tuning. Nature 376, 236–238.

Cousins, S., Cutfield, N.J., Kaski, D., Palla, A., Seemungal, B.M., Golding, J.F., Staab, J.P., Bronstein, A.M., 2014. Visual dependency and dizziness after vestibular neuritis. PLoS One 9, e105426.

Cousins, S., Kaski, D., Cutfield, N., Arshad, Q., Ahmad, H., Gresty, M.A., Seemungal, B.M., Golding, J., Bronstein, A.M., 2017. Predictors of clinical recovery from vestibular neuritis: a prospective study. Ann. Clin. Transl. Neurol. 4, 340–346.

Cutfield, N.J., Scott, G., Waldman, A.D., Sharp, D.J., Bronstein, A.M., 2014. Visual and proprioceptive interaction in patients with bilateral vestibular loss. Neuroimage Clin. 4, 274–282.

Cyran, C.A., Boegle, R., Stephan, T., Dieterich, M., Glasauer, S., 2016. Age-related decline in functional connectivity of the vestibular cortical network. Brain Struct. Funct. 221, 1443–1463.

Deutschlander, A., Hufner, K., Kalla, R., Stephan, T., Dera, T., Glasauer, S., Wiesmann, M., Strupp, M., Brandt, T., 2008. Unilateral vestibular failure suppresses cortical visual motion processing. Brain 131, 1025–1034.

Dieterich, M., Brandt, T., 2008. Functional brain imaging of peripheral and central vestibular disorders. Brain 131, 2538–2552.

Dieterich, M., Bauermann, T., Best, C., Stoeter, P., Schlindwein, P., 2007. Evidence for cortical visual substitution of chronic bilateral vestibular failure (an fMRI study). Brain 130, 2108–2116.

Eickhoff, S.B., Stephan, K.E., Mohlberg, H., Grefkes, C., Fink, G.R., Amunts, K., Zilles, K., 2005. A new SPM toolbox for combining probabilistic cytoarchitectonic maps and functional imaging data. Neuroimage 25, 1325–1335.

Eickhoff, S.B., Paus, T., Caspers, S., Grosbras, M.H., Evans, A.C., Zilles, K., Amunts, K., 2007. Assignment of functional activations to probabilistic cytoarchitectonic areas revisited. Neuroimage 36, 511–521.

Ertl, M., Klimek, M., Boegle, R., Stephan, T., Dieterich, M., 2018 Oct. Vestibular perception thresholds tested by galvanic vestibular stimulation. J. Neurol. 265 (Suppl 1), 54–56. https://doi.org/10.1007/s00415-018-8808-9.

Fetsch, C.R., Turner, A.H., DeAngelis, G.C., Angelaki, D.E., 2009. Dynamic reweighting of visual and vestibular cues during self-motion perception. J. Neurosci. 29, 15601–15612.

Fitzpatrick, R.C., Day, B.L., 2004. Probing the human vestibular system with galvanic stimulation. J. Appl. Physiol. 96, 2301–2316.

Fitzpatrick, R.C., Wardman, D.L., Taylor, J.L., 1999. Effects of galvanic vestibular stimulation during human walking. J. Physiol. 517 (Pt 3), 931–939.

Fitzpatrick, R.C., Marsden, J., Lord, S.R., Day, B.L., 2002. Galvanic vestibular stimulation evokes sensations of body rotation. Neuroreport 13, 2379–2383.

Fornos, A.P., Cavuscens, S., Ranieri, M., van de Berg, R., Stokroos, R., Kingma, H., Guyot, J.P., Guinand, N., 2017. The vestibular implant: a probe in orbit around the human balance system. J. Vestib. Res. Equilib. Orient. 27, 51–61.

Fujimoto, C., Yamamoto, Y., Kamogashira, T., Kinoshita, M., Egami, N., Uemura, Y., Togo, F., Yamasoba, T., Iwasaki, S., 2016. Noisy galvanic vestibular stimulation induces a sustained improvement in body balance in elderly adults. Sci. Rep. 6, 37575.

Fujimoto, C., Egami, N., Kawahara, T., Uemura, Y., Yamamoto, Y., Yamasoba, T., Iwasaki, S., 2018. Noisy galvanic vestibular stimulation sustainably improves posture in bilateral vestibulopathy. Front. Neurol. 9, 900.

Galletti, C., Gamberini, M., Kutz, D.F., Fattori, P., Luppino, G., Matelli, M., 2001. The cortical connections of area V6: an occipito-parietal network processing visual information. Eur. J. Neurosci. 13, 1572–1588.

Gensberger, K.D., Kaufmann, A.K., Dietrich, H., Branoner, F., Banchi, R., Chagnaud, B.P., Straka, H., 2016. Galvanic vestibular stimulation: cellular substrates and response patterns of neurons in the vestibulo-ocular network. J. Neurosci. 36, 9097–9110.

Gläscher, J., 2008. Contrast Weights in Flexible Factorial Design with Multiple Groups of Subjects.

Goel, R., Kofman, I., Jeevarajan, J., De Dios, Y., Cohen, H.S., Bloomberg, J.J., Mulavara, A.P., 2015. Using low levels of stochastic vestibular stimulation to improve balance function. PLoS One 10, e0136335.

Gottlich, M., Jandl, N.M., Wojak, J.F., Sprenger, A., der Gablentz, J., Munte, T.F., Kramer, U.M., Helmchen, C., 2014. Altered resting-state functional connectivity in patients with chronic bilateral vestibular failure. Neuroimage Clin. 4, 488–499.

Gottlich, M., Jandl, N.M., Sprenger, A., Wojak, J.F., Munte, T.F., Kramer, U.M., Helmchen, C., 2016. Hippocampal gray matter volume in bilateral vestibular failure. Hum. Brain Mapp. 37, 1998–2006.

Helfrich, R.F., Becker, H.G., Haarmeier, T., 2013. Processing of coherent visual motion in topographically organized visual areas in human cerebral cortex. Brain Topogr. 26, 247–263.

Helmchen, C., Klinkenstein, J., Machner, B., Rambold, H., Mohr, C., Sander, T., 2009. Structural changes in the human brain following vestibular neuritis indicate central vestibular compensation. Ann. N. Y. Acad. Sci. 1164, 104–115.

Helmchen, C., Klinkenstein, J.C., Kruger, A., Gliemroth, J., Mohr, C., Sander, T., 2011. Structural brain changes following peripheral vestibulo-cochlear lesion may indicate multisensory compensation. J. Neurol. Neurosurg. Psychiatry 82, 309–316.

Helmchen, C., Ye, Z., Sprenger, A., Munte, T.F., 2014. Changes in resting-state fMRI in vestibular neuritis. Brain Struct. Funct. 219, 1889–1900.

Helmchen, C., Knauss, J., Trillenberg, P., Frendl, A., Sprenger, A., 2017. Role of the Patient's history of vestibular symptoms in the clinical evaluation of the bedside head-impulse test. Front. Neurol. 8, 51.

Iwasaki, S., Yamamoto, Y., Togo, F., Kinoshita, M., Yoshifuji, Y., Fujimoto, C., Yamasoba, T., 2014. Noisy vestibular stimulation improves body balance in bilateral vestibulopathy. Neurology 82, 969–975.

Jorns-Haderli, M., Straumann, D., Palla, A., 2007. Accuracy of the bedside head impulse test in detecting vestibular hypofunction. J. Neurol. Neurosurg. Psychiatry 78, 1113–1118.

Kalla, R., Muggleton, N., Spiegel, R., Bueti, D., Claassen, J., Walsh, V., Bronstein, A.,

2011. Adaptive motion processing in bilateral vestibular failure. J. Neurol. Neurosurg. Psychiatry 82, 1212–1216.
Karim, H.T., Fuhrman, S.I., Furman, J.M., Huppert, T.J., 2013. Neuroimaging to detect cortical projection of vestibular response to caloric stimulation in young and older adults using functional near-infrared spectroscopy (fNIRS). Neuroimage 76, 1–10.
Kim, J.M., Mun, S.K., Yoo, I.H., Lopez, C., Kim, J.S., 2018. Vertigo and impaired pursuit eye movements in a small medial superior temporal infarction. J. Neurol. 265, 2740–2742.
Lobel, E., Kleine, J.F., Bihan, D.L., Leroy-Willig, A., Berthoz, A., 1998. Functional MRI of galvanic vestibular stimulation. J. Neurophysiol. 80, 2699–2709.
Lopez, C., Blanke, O., 2011. The thalamocortical vestibular system in animals and humans. Brain Res. Rev. 67, 119–146.
Machner, B., Sprenger, A., Fullgraf, H., Trillenberg, P., Helmchen, C., 2013. Video-based head impulse test. Importance for routine diagnostics of patients with vertigo. Nervenarzt 84, 975–983.
Moss, F., Ward, L.M., Sannita, W.G., 2004. Stochastic resonance and sensory information processing: a tutorial and review of application. Clin. Neurophysiol. 115, 267–281.
Pal, S., Rosengren, S.M., Colebatch, J.G., 2009. Stochastic galvanic vestibular stimulation produces a small reduction in sway in Parkinson's disease. J. Vestib. Res. 19, 137–142.
Roberts, R.E., Ahmad, H., Arshad, Q., Patel, M., Dima, D., Leech, R., Seemungal, B.M., Sharp, D.J., Bronstein, A.M., 2017. Functional neuroimaging of visuo-vestibular interaction. Brain Struct. Funct. 222, 2329–2343.
Roberts, R.E., Ahmad, H., Patel, M., Dima, D., Ibitoye, R., Sharif, M., Leech, R., Arshad, Q., Bronstein, A.M., 2018. An fMRI study of visuo-vestibular interactions following vestibular neuritis. Neuroimage Clin. 20, 1010–1017.
Rottschy, C., Eickhoff, S.B., Schleicher, A., Mohlberg, H., Kujovic, M., Zilles, K., Amunts, K., 2007. Ventral visual cortex in humans: cytoarchitectonic mapping of two extrastriate areas. Hum. Brain Mapp. 28, 1045–1059.
Ruhl, R.M., Bauermann, T., Dieterich, M., Zu Eulenburg, P., 2018. Functional correlate and delineated connectivity pattern of human motion aftereffect responses substantiate a subjacent visual-vestibular interaction. Neuroimage 174, 22–34.
Samoudi, G., Jivegard, M., Mulavara, A.P., Bergquist, F., 2015. Effects of stochastic vestibular galvanic stimulation and LDOPA on balance and motor symptoms in patients with Parkinson's disease. Brain Stimul. 8, 474–480.
Shallo-Hoffmann, J., Bronstein, A.M., 2003. Visual motion detection in patients with absent vestibular function. Vis. Res. 43, 1589–1594.
Sprenger, A., Wojak, J.F., Jandl, N.M., Hertel, S., Helmchen, C., 2014. Predictive mechanisms improve the vestibulo-ocular reflex in patients with bilateral vestibular failure. J. Neurol. 261, 628–631.
Stephan, T., Deutschlander, A., Nolte, A., Schneider, E., Wiesmann, M., Brandt, T., Dieterich, M., 2005. Functional MRI of galvanic vestibular stimulation with alternating currents at different frequencies. Neuroimage 26, 721–732.
Strupp, M., Arbusow, V., Dieterich, M., Sautier, W., Brandt, T., 1998. Perceptual and oculomotor effects of neck muscle vibration in vestibular neuritis. Ipsilateral somatosensory substitution of vestibular function. Brain 121 (Pt 4), 677–685.
Strupp, M., Kim, J.S., Murofushi, T., Straumann, D., Jen, J.C., Rosengren, S.M., Della Santina, C.C., Kingma, H., 2017. Bilateral vestibulopathy: diagnostic criteria consensus document of the classification Committee of the Barany Society. J. Vestib. Res. 27, 177–189.
Tax, C.M., Bom, A.P., Taylor, R.L., Todd, N., Cho, K.K., Fitzpatrick, R.C., Welgampola, M.S., 2013. The galvanic whole-body sway response in health and disease. Clin. Neurophysiol. 124, 2036–2045.
Tschan, R., Wiltink, J., Best, C., Beutel, M., Dieterich, M., Eckhardt-Henn, A., 2010. Validation of the German version of the Vertigo handicap questionnaire (VHQ) in patients with vestibular vertigo syndromes or somatoform vertigo and dizziness. Psychother. Psychosom. Med. Psychol. 60, e1–12.
Tzourio-Mazoyer, N., Landeau, B., Papathanassiou, D., Crivello, F., Etard, O., Delcroix, N., Mazoyer, B., Joliot, M., 2002. Automated anatomical labeling of activations in SPM using a macroscopic anatomical parcellation of the MNI MRI single-subject brain. Neuroimage 15, 273–289.
Ventre-Dominey, J., 2014. Vestibular function in the temporal and parietal cortex: distinct velocity and inertial processing pathways. Front. Integr. Neurosci. 8, 53.
Volkening, K., Bergmann, J., Keller, I., Wuehr, M., Muller, F., Jahn, K., 2014. Verticality perception during and after galvanic vestibular stimulation. Neurosci. Lett. 581, 75–79.
Wilkinson, D., Zubko, O., Sakel, M., Coulton, S., Higgins, T., Pullicino, P., 2014. Galvanic vestibular stimulation in hemi-spatial neglect. Front. Integr. Neurosci. 8, 4.
Wuehr, M., Nusser, E., Decker, J., Krafczyk, S., Straube, A., Brandt, T., Jahn, K., Schniepp, R., 2016a. Noisy vestibular stimulation improves dynamic walking stability in bilateral vestibulopathy. Neurology 86, 2196–2202.
Wuehr, M., Nusser, E., Krafczyk, S., Straube, A., Brandt, T., Jahn, K., Schniepp, R., 2016b. Noise-enhanced vestibular input improves dynamic walking stability in healthy subjects. Brain Stimul. 9, 109–116.
Wuehr, M., Boerner, J.C., Pradhan, C., Decker, J., Jahn, K., Brandt, T., Schniepp, R., 2018. Stochastic resonance in the human vestibular system - noise-induced facilitation of vestibulospinal reflexes. Brain Stimul. 11, 261–263.
Zingler, V.C., Cnyrim, C., Jahn, K., Weintz, E., Fernbacher, J., Frenzel, C., Brandt, T., Strupp, M., 2007. Causative factors and epidemiology of bilateral vestibulopathy in 255 patients. Ann. Neurol. 61, 524–532.
Zingler, V.C., Weintz, E., Jahn, K., Mike, A., Huppert, D., Rettinger, N., Brandt, T., Strupp, M., 2008. Follow-up of vestibular function in bilateral vestibulopathy. J. Neurol. Neurosurg. Psychiatry 79, 284–288.
zu Eulenburg, P., Stoeter, P., Dieterich, M., 2010. Voxel-based morphometry depicts central compensation after vestibular neuritis. Ann. Neurol. 68, 241–249.
Zu Eulenburg, P., Caspers, S., Roski, C., Eickhoff, S.B., 2011. Meta-analytical definition and functional connectivity of the human vestibular cortex. Neuroimage 60, 162–169.
zu Eulenburg, P., Muller-Forell, W., Dieterich, M., 2013. On the recall of vestibular sensations. Brain Struct. Funct. 218, 255–267.